




## Article

# Deep Eutectic Solvent Coated Cerium Oxide Nanoparticles Based Polysulfone Membrane to Mitigate Environmental Toxicology

Saif-ur-Rehman <sup>1,2,\*</sup> , Muhammad Shozab Mehdi <sup>3,\*</sup>, Muhammad Fakhar-e-Alam <sup>4</sup>, Muhammad Asif <sup>4</sup>, Javed Rehman <sup>5,6,7</sup>, Razan A. Alshgari <sup>8</sup>, Muddasar Jamal <sup>1,2,9</sup>, Shafiq Uz Zaman <sup>3</sup> , Muhammad Umar <sup>3</sup>, Sikander Rafiq <sup>10</sup>, Nawshad Muhammad <sup>11</sup>, Junaid bin Fawad <sup>1</sup> and Saiful Arifin Shafiee <sup>6</sup> 

- <sup>1</sup> Department of Chemical Engineering, COMSATS University Islamabad, Lahore Campus, Defence Road, Off Raiwind Road, Lahore 54000, Punjab, Pakistan; muddasar\_18002825@utp.edu.my (M.J.); gourmani5@yahoo.com (J.b.F.)
- <sup>2</sup> Interdisciplinary Research Center in Biomedical Materials, COMSATS University Islamabad, Lahore Campus, Defence Road, Off Raiwind Road, Lahore 54000, Punjab, Pakistan
- <sup>3</sup> Department of Chemical Engineering, Ghulam Ishaq Khan Institute of Engineering Sciences and Technology, Topi 23460, Khyber Pakhtunkhwa, Pakistan; shafiqzaman029@gmail.com (S.U.Z.); umardurrani07@gmail.com (M.U.)
- <sup>4</sup> Department of Physics, GC University Faisalabad, Faisalabad 38000, Punjab, Pakistan; fakharphy@gmail.com (M.F.-e.-A.); asif3220286@gmail.com (M.A.)
- <sup>5</sup> State Key Laboratory of Metastable Materials Science and Technology, School of Materials Science and Engineering, Yanshan University, Qinhuangdao 066004, China; javed\_rehman15@yahoo.com
- <sup>6</sup> Department of Chemistry, Kuliyah of Science, International Islamic University, Malaysia, Jalan Sultan Ahmad Shah, Kuantan 25200, Pahang, Malaysia; sabs@iiu.edu.my
- <sup>7</sup> MEU Research Unit, Middle East University, Amman 541350, Jordan
- <sup>8</sup> Chemistry Department, College of Science, King Saud University, Riyadh 11451, Saudi Arabia; ralshgari@ksu.edu.sa
- <sup>9</sup> Department of Chemical Engineering, Universiti Teknologi PETRONAS, Bandar Seri Iskandar 32610, Perak, Malaysia
- <sup>10</sup> Department of Chemical, Polymer and Composite Materials Engineering, University of Engineering and Technology Lahore, New Campus, Lahore 39161, Punjab, Pakistan; sikander@uet.edu.pk
- <sup>11</sup> Department of Dental Materials, Institute of Basic Medical Sciences, Khyber Medical University, Peshawar 25100, Khyber Pakhtunkhwa, Pakistan; nawshad.ibms@kmu.edu.pk
- \* Correspondence: saifzciit@gmail.com (S.-u.-R.); shozab@giki.edu.pk (M.S.M.)



**Citation:** Saif-ur-Rehman; Shozab Mehdi, M.; Fakhar-e-Alam, M.; Asif, M.; Rehman, J.; A. Alshgari, R.; Jamal, M.; Uz Zaman, S.; Umar, M.; Rafiq, S.; et al. Deep Eutectic Solvent Coated Cerium Oxide Nanoparticles Based Polysulfone Membrane to Mitigate Environmental Toxicology. *Molecules* **2023**, *28*, 7162. <https://doi.org/10.3390/molecules28207162>

Academic Editor: Xingang Liu

Received: 12 September 2023

Revised: 4 October 2023

Accepted: 11 October 2023

Published: 19 October 2023



**Copyright:** © 2023 by the authors. Licensee MDPI, Basel, Switzerland. This article is an open access article distributed under the terms and conditions of the Creative Commons Attribution (CC BY) license (<https://creativecommons.org/licenses/by/4.0/>).

**Abstract:** In this study, ceria nanoparticles (NPs) and deep eutectic solvent (DES) were synthesized, and the ceria-NP's surfaces were modified by DES to form DES-ceria NP filler to develop mixed matrix membranes (MMMs). For the sake of interface engineering, MMMs of 2%, 4%, 6% and 8% filler loadings were fabricated using solution casting technique. The characterizations of SEM, FTIR and TGA of synthesized membranes were performed. SEM represented the surface and cross-sectional morphology of membranes, which indicated that the filler is uniformly dispersed in the polysulfone. FTIR was used to analyze the interaction between the filler and support, which showed there was no reaction between the polymer and DES-ceria NPs as all the peaks were consistent, and TGA provided the variation in the membrane materials with respect to temperature, which categorized all of the membranes as very stable and showed that the trend of stability increases with respect to DES-ceria NPs filler loading. For the evaluation of efficiency of the MMMs, the gas permeation was tested. The permeability of CO<sub>2</sub> was improved in comparison with the pristine Polysulfone (PSF) membrane and enhanced selectivities of 35.43 ( $\alpha_{\text{CO}_2/\text{CH}_4}$ ) and 39.3 ( $\alpha_{\text{CO}_2/\text{N}_2}$ ) were found. Hence, the DES-ceria NP-based MMMs proved useful in mitigating CO<sub>2</sub> from a gaseous mixture.

**Keywords:** interface engineering; deep eutectic solvents; ceria nanoparticles; membranes; gas separation

## 1. Introduction

CO<sub>2</sub> is the major impurity found in natural gas, which is a major contributor to methane and is an important source of renewable energy [1]. The CO<sub>2</sub> in natural gas causes the corrosion of pipelines and reduces its calorific value [2]. Also, as it is a greenhouse gas, it results in a thermal effect on the environment by absorbing radiation which gives rise to global warming. Concerning the sources of CO<sub>2</sub> emissions, power generation is the major CO<sub>2</sub> discharge source, which is due to the combustion of natural gas and coal or other fossil fuels for the production of electricity [3]. The burning of fuels in vehicles on a domestic level, as well as in other industries, are further sources of CO<sub>2</sub> emissions. Hence, to reduce greenhouse gas emissions and global warming, to improve economic efficiency, and to provide a sustainable source of energy, it has become necessary to separate CO<sub>2</sub> from natural gas [4]. As well as CO<sub>2</sub>/CH<sub>4</sub> separation, CO<sub>2</sub>/N<sub>2</sub> separation is also necessary as it improves the cleanliness of the atmosphere and reduces the percentage of CO<sub>2</sub> in the environment [5].

Membrane technology has attracted researchers due to its attributes of having a small footprint, being easy to operate and having a low energy consumption in separating CO<sub>2</sub> [6]. Membrane-based materials have great significance in this field [7] and organic polymeric membranes are leading the market, as compared to other two-dimensional materials [8] and organics [9–11]. The reasons for this are the low cost, easy processing, and high mechanical strength of the polymers [12,13]. The major problem faced in this field is overcoming the permeability and selectivity trade-off as explained by Robeson [14]. The incorporation of novel advanced fillers on polymeric support to synthesize membranes may provide an effective solution to optimize the perm-selectivity trade-off [15,16].

The synthesis of mixed matrix membranes (MMMs) has some drawbacks, like fewer interactions between filler particles and polymers, the non-uniform dispersion of the filler on polymer, and chances of a reaction between the filler and polymers [17,18]. The interface morphology of MMMs is also a significant factor in separation via membrane and is controlled by novel supervenient materials as filler. Covalent organic frameworks (COFs), metal organic frameworks (MOFs), metal oxides, alumina, silica, zeolites, nanoparticles, nanographenes, and ceramics are the materials that are being used as filler for CO<sub>2</sub> separation in different separation techniques, as well as in the fabrication of MMMs [19–21]. Sometimes inimical problems occur due to an acidic or humid environment, which can become the cause of interface incompatibility between the filler and polymer [22]. The specification of the filler plays a key role in overcoming this type of problem, and desirable features can be imparted to the membranes by introducing specific fillers in the membrane matrix [23,24].

Recent studies have employed nanoparticles as the filler in mixed matrix membranes. Hasebe et al. [25] has applied silica nanoparticles in polymeric membranes to separate CO<sub>2</sub> as a way to overcome the Robeson upper bound limit, which resulted in a cost-effective solution for high performance CO<sub>2</sub> separation in the form of permeability and selectivity (CO<sub>2</sub>/N<sub>2</sub>) on large scale. Raouf et al. [26] have used graphene hydroxyl nanoparticles and polysulfone/polyethylene glycol to synthesize MMMs and obtained a permeability in the range of 15.9–28.2 Barrer and a selectivity (CO<sub>2</sub>/CH<sub>4</sub>) range of 12.23–12.81 at 2 bar pressure with a maximum of 22.39 at 8 bar pressure. Sainath et al. [27] grew ZIF-67 NPs on PSF/GO hollow fiber membranes (HFMs) to increase the CO<sub>2</sub> removal from natural gas and reported selectivities of  $44.94 \pm 3.00$  and  $22.38 \pm 0.30$  for mixed and pure, respectively. Ruhaimi et al. [28] synthesized spherical CeO<sub>2</sub> nanoparticles to apply in egg-shell membranes as a bio-template for the high efficiency of CO<sub>2</sub> adsorption. Farashi et al. [29] has improved CO<sub>2</sub> separation from CH<sub>4</sub> using a Pebax-1657 membrane with the addition of alumina (Al<sub>2</sub>O<sub>3</sub>) NPs in the membrane matrix and reported CO<sub>2</sub> permeability as 159.27 Barrer and selectivity as 24.73 at 8% Al<sub>2</sub>O<sub>3</sub> NP loadings by weight with different characterizations of membrane. And Xu et al. [30] reported the high NPs loadings in MMMs with the help of chemical bridging-crosslinking for the high performance separation of CO<sub>2</sub> and found the permeation of CO<sub>2</sub> and selectivity (CO<sub>2</sub>/N<sub>2</sub>) to be 1295 GPU and 91 at 0.3 MPa, respectively.

In this study, the purpose was to mitigate the amount of CO<sub>2</sub> from the gaseous mixture to reduce the toxicity of the gases, like natural gas, flue gases etc. A lot of materials have been used for this purpose, so there was the need to make a novel combination of the compounds that could have the potential to give better outcomes for this purpose. Following this purpose, DES immobilized cerium oxide (CeO<sub>2</sub>) is used in MMMs for CO<sub>2</sub> separation. DESs are popular candidates and green solvents in the membrane technology because of their nontoxicity, low viscosity, low vapor pressure, prominent tunability, easy preparation, high biocompatibility and biodegradability [31]. It can be synthesized by mixing and heating at least two chemicals that are hydrogen bond donors (HBD) and hydrogen bond acceptors (HBA) [32]. Therefore, DES was synthesized by cetrimonium bromide (CTMB) and acetic acid as HBA and HBD, respectively. The nanoparticles (NPs) of ceria were synthesized by using cerium (IV) ammonium nitrate, ethylene glycol and isopropanol. DES was immobilized on ceria NPs by using ethanol via a solvent evaporation technique and filler for the MMMs was obtained. Polysulfone was used as support material to maintain the strength of the membrane matrix as it is easy to process, mechanically strong, and thermally and chemically stable. Finally, mixed matrix membranes of 2%, 4%, 6% and 8% DES immobilized ceria NP loadings were synthesized and analyzed by FTIR, SEM and TGA. Also, gas permeation was evaluated on the permeation of CO<sub>2</sub> and the selectivities of CO<sub>2</sub>/N<sub>2</sub> and CO<sub>2</sub>/CH<sub>4</sub> for the detection of CO<sub>2</sub> mitigation from the gaseous mixture. The results obtained proved that this combination tries to overcome and to optimize the trade-off between permeability and selectivity in the Robeson plot and lie near the line that might be a potential region of the plot. No doubt, it was not able to completely overcome the Robeson upper bound limit, but it still has potential improvement to be reported in comparison with pure polysulfone membranes.

## 2. Results and Discussion

### 2.1. Scanning Electron Microscopy (SEM)

SEM (Tescan Vega (LMU)) was utilized to observe the cross-sectional and surface morphology of the membranes of different NP loadings (Figures 1 and S1). Membranes were broken in liquid nitrogen to fix the cross-sectional ends of the membranes and a voltage of 15–20 Kv at different magnifications was applied with gold coating of the samples in the SEM machine. A SEM micrograph is used to observe the aggregation, dispersion and the existence of the filler NPs in the membrane matrix. SEM images show the increasing NP loadings as 2%, 4%, 6% and 8% in the membrane and the filler is highly dispersed across the whole membrane in each case. All of the membranes are accurately synthesized, and the structural density of the composition is visible without any imperfections. Some of the ripples can be seen with the increase of filler loadings that are due to inert NP aggregation that leads to agglomeration in greater than 8% NP loadings. Obviously, the nanoparticles form agglomerates due to the strong interaction between the modified small particles which can be a consequence of generating channels or voids that indicate the molecular chains' flexibility in the membrane matrix [33]. The agglomeration is also due to the fact that the shape of the DES-modified ceria NPs cannot be assumed [34]. The main contribution of the selective gas permeation and membrane strength depends upon the pore structure of MMMs [35], which is obvious from the cross-section morphology. The springy asymmetric structures shown are due to the strong contact between the filler and polysulfone, and poor attraction of tetrahydrofuran (THF), which is the organic solvent that caused the skin-like structures while drying [36]. Hence the uniform and homogeneous dispersion of the filler exhibited by the images point towards the enhanced permeation of CO<sub>2</sub> and the relative selectivities. The pore formation increases with the increase of DES-ceria which supports the hypothesis.

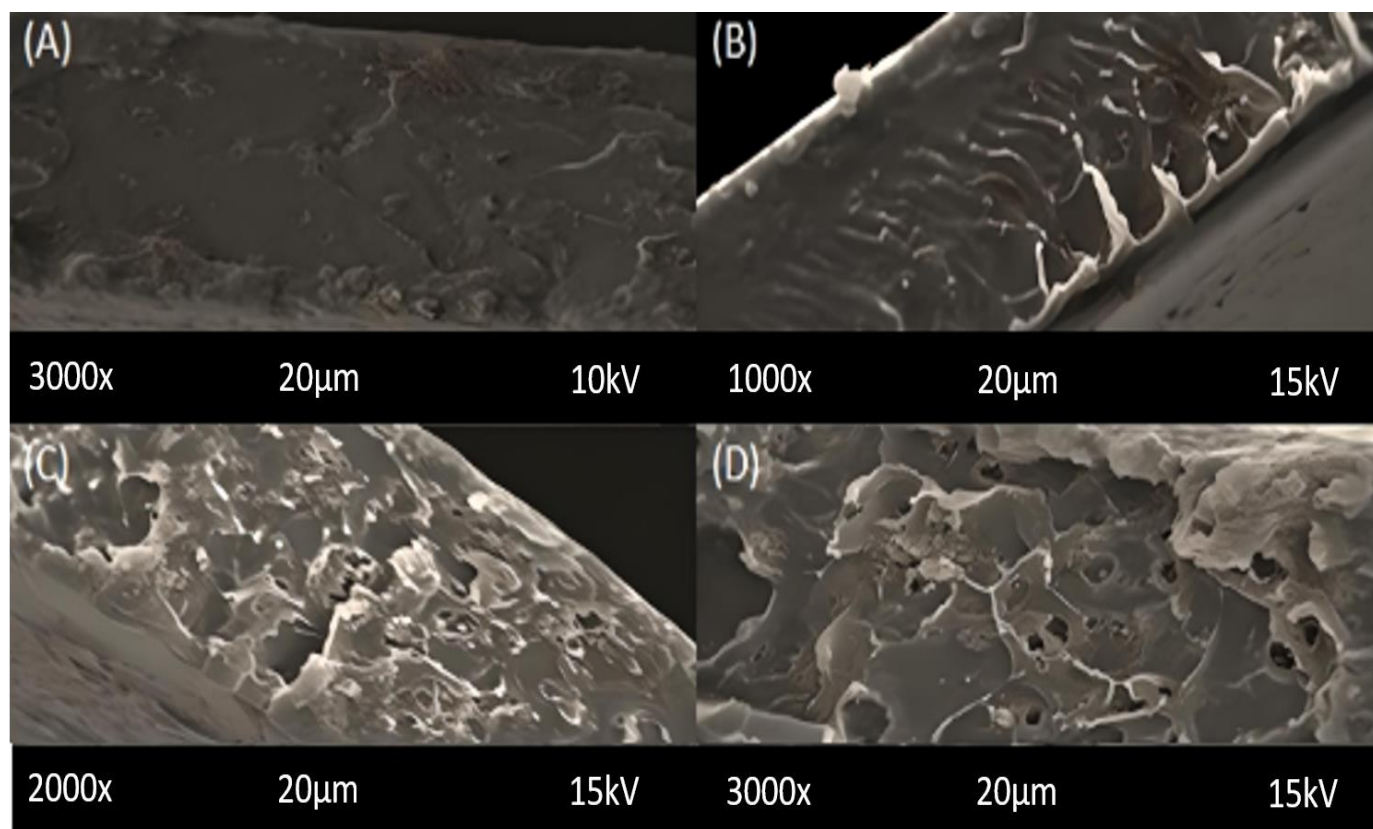


**Figure 1.** SEM images of cross-sections of MMMs of different filler loadings (A) 2% (B) 4% (C) 6% (D) 8%.

## 2.2. Fourier Transform Infrared (FTIR) Spectroscopy

Figure 2 demonstrates the FTIR spectra for ceria, DES-immobilized ceria and all of the four compositions of the membranes in a  $650\text{--}1800\text{ cm}^{-1}$  range. The major peak of ceria, that is the O-Ce-O stretching vibration, is at  $1071\text{ cm}^{-1}$  [37–39]. It can be observed in all of the membrane compositions that indicated the presence of ceria filler in the synthesized MMMs. The peak at  $1582\text{ cm}^{-1}$  indicates C=C stretching vibrations and benzene ring stretching [40]. The peaks at  $1291\text{ cm}^{-1}$ ,  $1321\text{ cm}^{-1}$  and  $1483\text{ cm}^{-1}$  are the peaks of symmetric O=S=O stretching vibrations and C-H bending vibrations. The peaks at  $1168\text{ cm}^{-1}$  shows C-O bending vibrations. The vibrational elongating symmetric behavior and asymmetric stretching vibrations of O=S=O bonds is represented by peaks at  $1101\text{ cm}^{-1}$  and at  $1146\text{ cm}^{-1}$ , respectively, which is a clear indication that sulfone groups exist. The peak at  $1233\text{ cm}^{-1}$  is a clear exhibition of the elongating vibration of Benz-O-Benz bonds, where Benz represents the benzene rings/aromatic functional group of PSF. The C=C stretching mode in aromatic compounds lies in the range  $1485\text{--}1590\text{ cm}^{-1}$ , which covers the peak at  $1503\text{ cm}^{-1}$ . The peak near  $1710\text{ cm}^{-1}$ , that is  $1740\text{ cm}^{-1}$ , indicates the symmetric stretching of a C=O bond, and at  $829\text{ cm}^{-1}$  indicates the  $\text{C}_6\text{H}_6$  ring bending. The peak at  $1010\text{ cm}^{-1}$  represents C-H stretching of the  $\text{C}_6\text{H}_6$  ring in PSF. The small shift in the peaks of the membrane in comparison with ceria NPs indicates the strong interface of the filler and polymer at the molecular level. A summary of all the peaks found can be seen in Table 1.

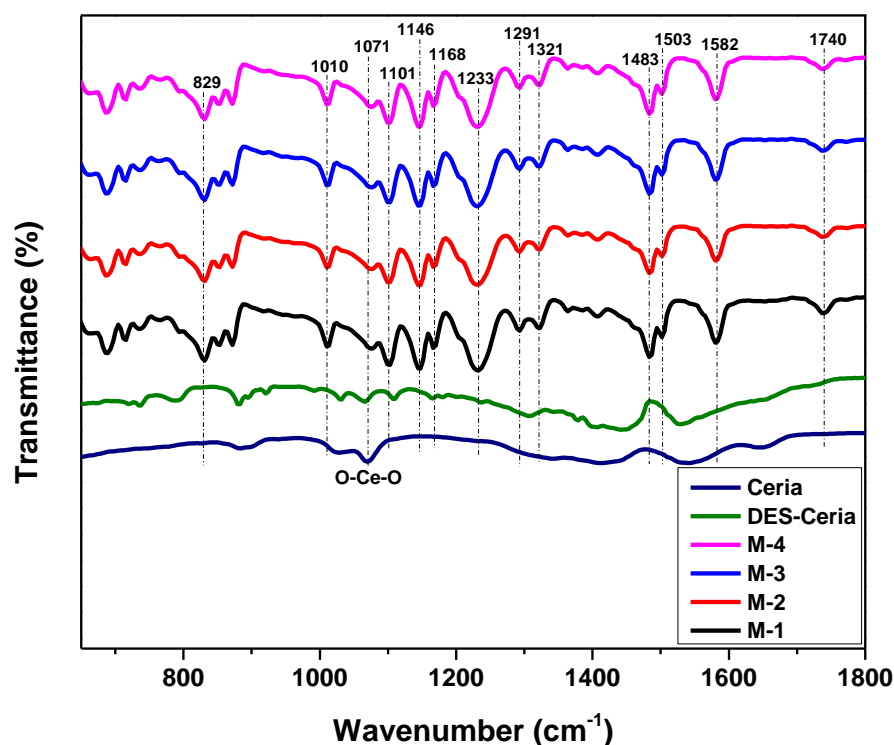


Figure 2. FTIR spectra for the ceria, DES-ceria and membrane compositions.

Table 1. Summary of FTIR spectra.

| Sr No. | Wavenumber (cm <sup>-1</sup> ) | Functional Groups   |
|--------|--------------------------------|---|
| 1      | 829                            | Benzene ring bending  |
| 2      | 1010                           | C-H stretching in benzene ring  |
| 3      | 1071                           | O-Ce-O stretching vibration   |
| 4      | 1101                           | Symmetric elongating vibration of O=S=O   |
| 5      | 1146                           | Asymmetric stretching vibration of O=S=O  |
| 6      | 1168                           | Bending vibration of C-O  |
| 7      | 1233                           | Elongating vibration of -C <sub>6</sub> H <sub>4</sub> -O-C <sub>6</sub> H <sub>4</sub> - |
| 8      | 1291, 1321                     | Symmetric stretching vibration of O=S=O   |
| 9      | 1483                           | Bending vibration of C-H  |
| 10     | 1503, 1582                     | Stretching mode of C=C in aromatics   |
| 11     | 1740                           | Symmetric stretching of C=O   |

### 2.3. Thermogravimetric Analysis

The thermogravimetric analysis was performed using a TGA analyzer (Perkin-Elmer STA 6000, Waltham, MA, USA), which is shown in Figure 3a, and the differential thermogravimetry is shown in Figure 3b to assess the thermal stability of MMMs. The MMMs were cut with a sample weight of 10 mg and placed in an oven at 100 °C to get rid of the enduring solvents and moisture, and then were cooled to room temperature. The cooled samples were placed in a sample holder and the temperature was adapted from 30 °C to 800 °C under a N<sub>2</sub> environment with a 10 °C/min heating rate. The TGA is better than other isothermal conventional methods for the evaluation of thermal decomposition; this is because very small amounts of the sample are enough for the investigation. All of the MMMs were found to be stable up to approximately 500 °C, which is an indication of quite high stability and the complex behavior of the TGA curves indicate the presence of multiple aromatic rings. The initial flatness of the curves is an indication of the removal of residual solvents, like THF, used in the synthesis process. The first 6% loss in the range of 110–230 °C leads to the amputation of the molecules. The further 4% decomposition between 230 °C to 500 °C represents decomposition of DES-ceria NPs, as the variations in the curves started



with the change of composition which represents the increase of thermal stability with the increase of DES-ceria NPs filler loading. This improvement of thermal stability proves the strong interaction between DES-ceria NPs and the polymer matrix. The sudden weight loss after 500 °C demonstrates breakage of the structure of major aromatic portions of PSF [33]. The normal temperature of flue gases is not more than 100 °C [30,41,42], hence it is right to say that MMMs are suitable for the capturing of CO<sub>2</sub> from flue gases under operating temperatures. All of these weight losses can also be observed in the DTG curves. These results are similar to other already reported studies [29,43–45].

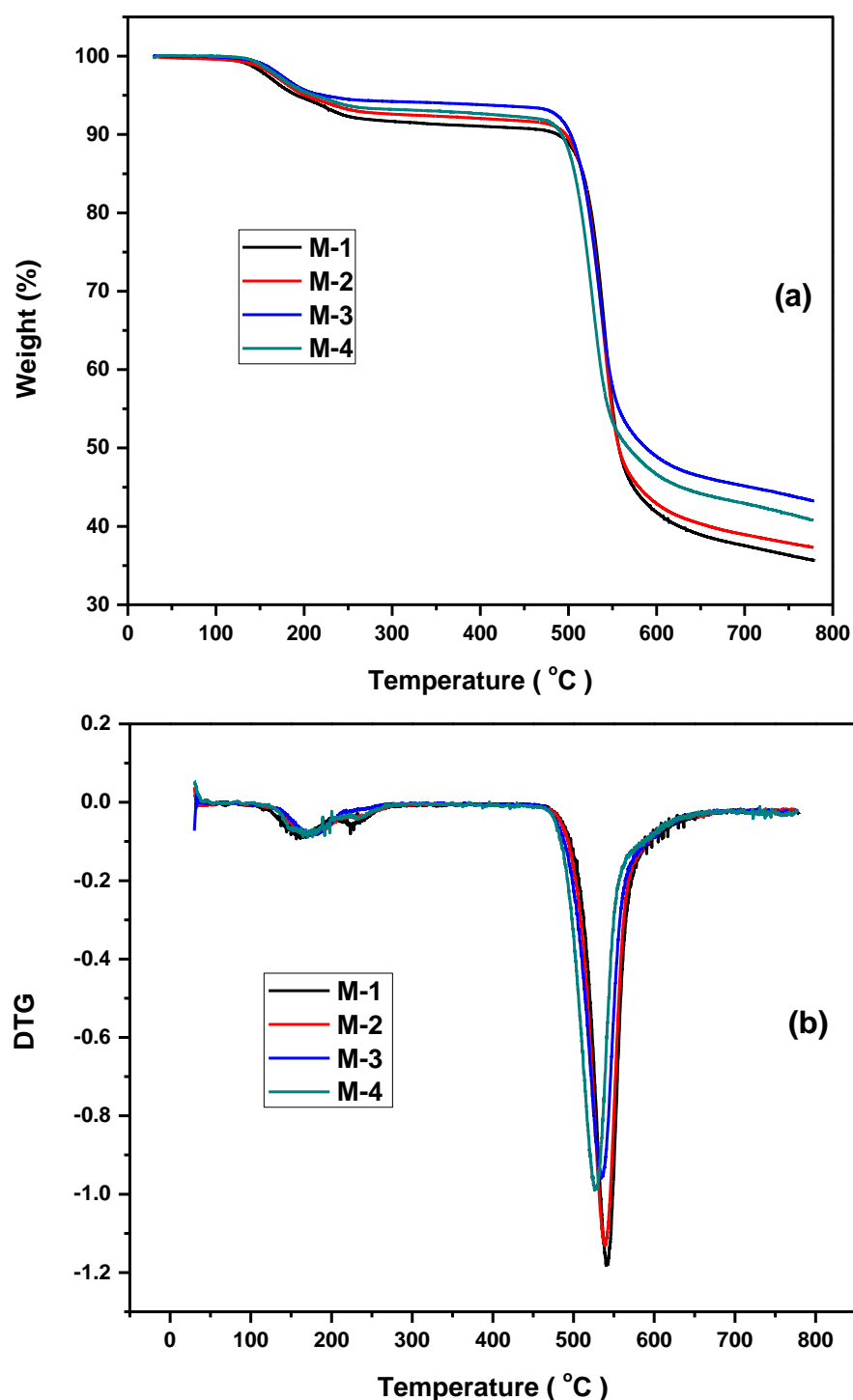


**Figure 3.** (a) Thermogravimetric analysis of membrane compositions. (b) Differential thermogravimetric analysis of membranes.

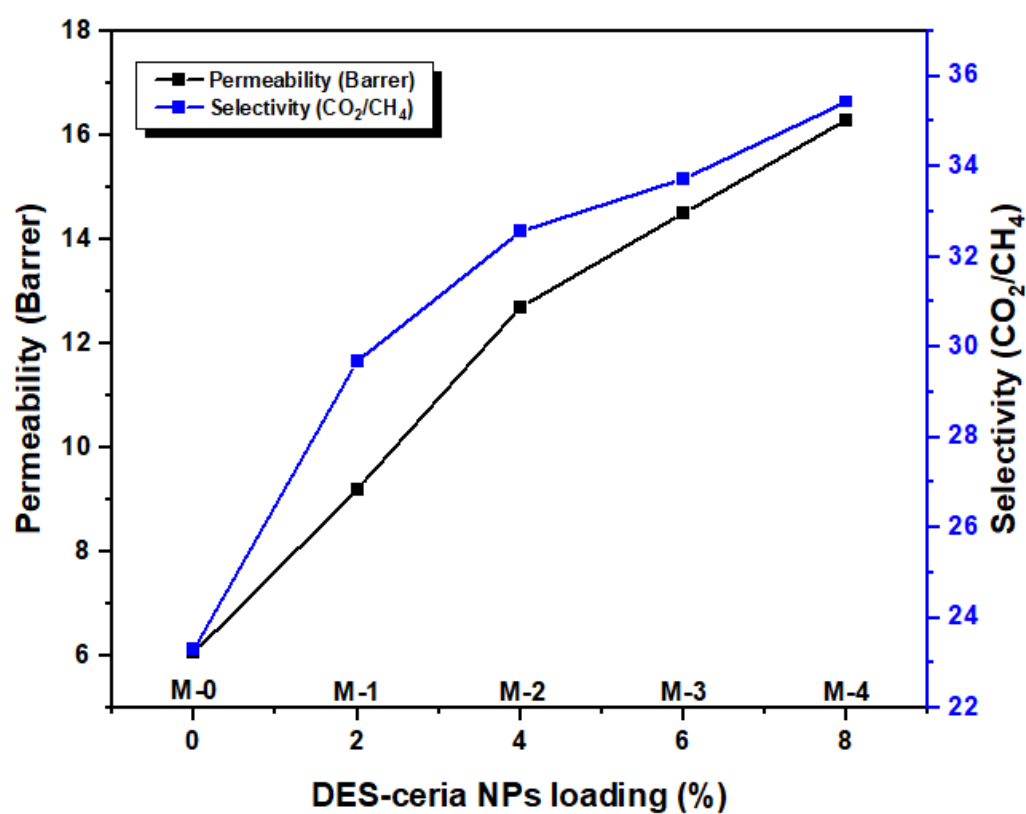
#### 2.4. Gas Permeation Analysis

The permeation of gases was evaluated using a custom-built system for analyzing the permeabilities and selectivities of mixed and pure gases. Permeate and retentate compositions were estimated with the help of a gas chromatograph (Agilent 7890, Santa Clara, CA, USA) that has twin thermal conductivity detectors. The overall scheme of the gas infiltration process has been reported elsewhere, as well as the construction and working of the setup [46]. Metallic support was utilized to place the membranes and seal them. The inlet gas mixture flow rate was 1 L/min. For membrane testing, the feed temperature and pressure of the system was kept at 25 °C and 10 bar. All of the measurements were taken a minimum of three times and average values were calculated. The solution-diffusion model was utilized for the transport mechanism via MMMs.

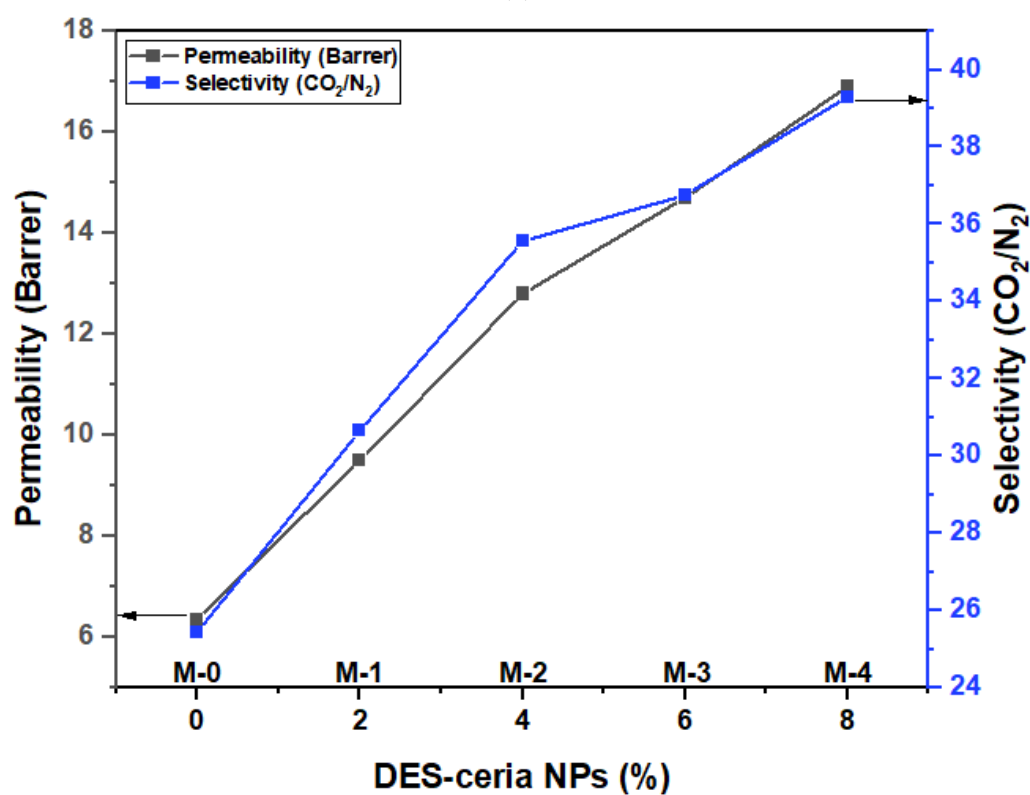
The permeabilities of CO<sub>2</sub> and the selectivities (CO<sub>2</sub>/CH<sub>4</sub> and CO<sub>2</sub>/N<sub>2</sub>) as a function of DES-ceria nanoparticle filler loadings are depicted in the Figure 4a,b. The variation in the permeabilities of different membrane compositions in comparison with pristine PSF membrane is termed as the facilitation ratio (FR). The FR is enhanced with the rise of filler from 2% to 4% DES-ceria NPs. The gas with smaller kinetic data (CO<sub>2</sub> = 3.3 Å) and a greater affinity with the amine and carboxyl groups present in DES exhibited an increased FR in comparison with gases of higher kinetic diameter (N<sub>2</sub> = 3.64 Å and CH<sub>4</sub> = 3.8 Å), which have a negligible affinity with the constituent functional groups of DES. This suggests that these results, within the same filler loading range, are due to the increment in pore density and the loss in pore size of membranes. The comparative study of the permeability of all three gases revealed the enhanced molecular sieving properties of DES-ceria NP-based MMMs that is the consequence of an overall increase in FR of CO<sub>2</sub>, N<sub>2</sub> and CH<sub>4</sub>; this has a minor effect on the non-selective gases and gave better separation of the selective gas CO<sub>2</sub>. Hence, we conclude that the existence of DES-supported ceria NPs enhanced the molecular sieving properties of the membranes and improved the whole process of CO<sub>2</sub> separation.

DES-ceria NP-based MMMs increased the CO<sub>2</sub> permeability from 6.06 Barrer to 16.3 Barrer and the selectivity from 23.31 to 35.43 in the case of CO<sub>2</sub>/CH<sub>4</sub> mixed gas. CO<sub>2</sub> permeability increased from 6.36 Barrer to 16.9 Barrer and the selectivity from 25.44 to 39.3 in the case of CO<sub>2</sub>/N<sub>2</sub> mixed gas. This is the FR of the gas permeation results. The difference between the results of the pure and mixed gases can be seen in Tables S1 and S2. This difference occurs because of the formation of the non-selective channels in MMMs. The incorporation of unambiguous functional groups was attempted to enhance CO<sub>2</sub> separation from the mixed gases with MMMs, due to the affinity of the amine and carboxyl groups towards CO<sub>2</sub>. Hence, this combination was highly efficient at separation without any high selectivity loss.

The results obtained from the permeation of gas analysis were calibrated with the famous Robeson plots as shown in the Figure 5a,b. The Robeson plot is an explanation of the association between permeability and selectivity, and it demonstrates the trade-off between these; if the permeability increases, the selectivity decreased; and if permeability decreases, the selectivity increases. The Robeson lines are considered the ideal lines for researchers to approach [14,29,47]. It is apparent that the points are moving towards the Robeson lines with respect to an increase in the filler loadings and the trade-off for the M-4 membrane is less than M-0. Therefore, in comparison with the pure PSF membrane, the 8% DES-ceria NP-based membrane has a smaller trade-off and lies in the technically strong region of the plot. Hence, the synthesized DES-ceria NP-based MMMs can be considered as potential candidates to enhance the efficiency of CO<sub>2</sub> separation from gaseous mixtures [48].



(a)



(b)

Figure 4. (a) Permeability and selectivity of MMMs for mixed gases  $\text{CO}_2/\text{CH}_4$ . (b) Permeability and selectivity of MMMs for mixed gases  $\text{CO}_2/\text{N}_2$ .



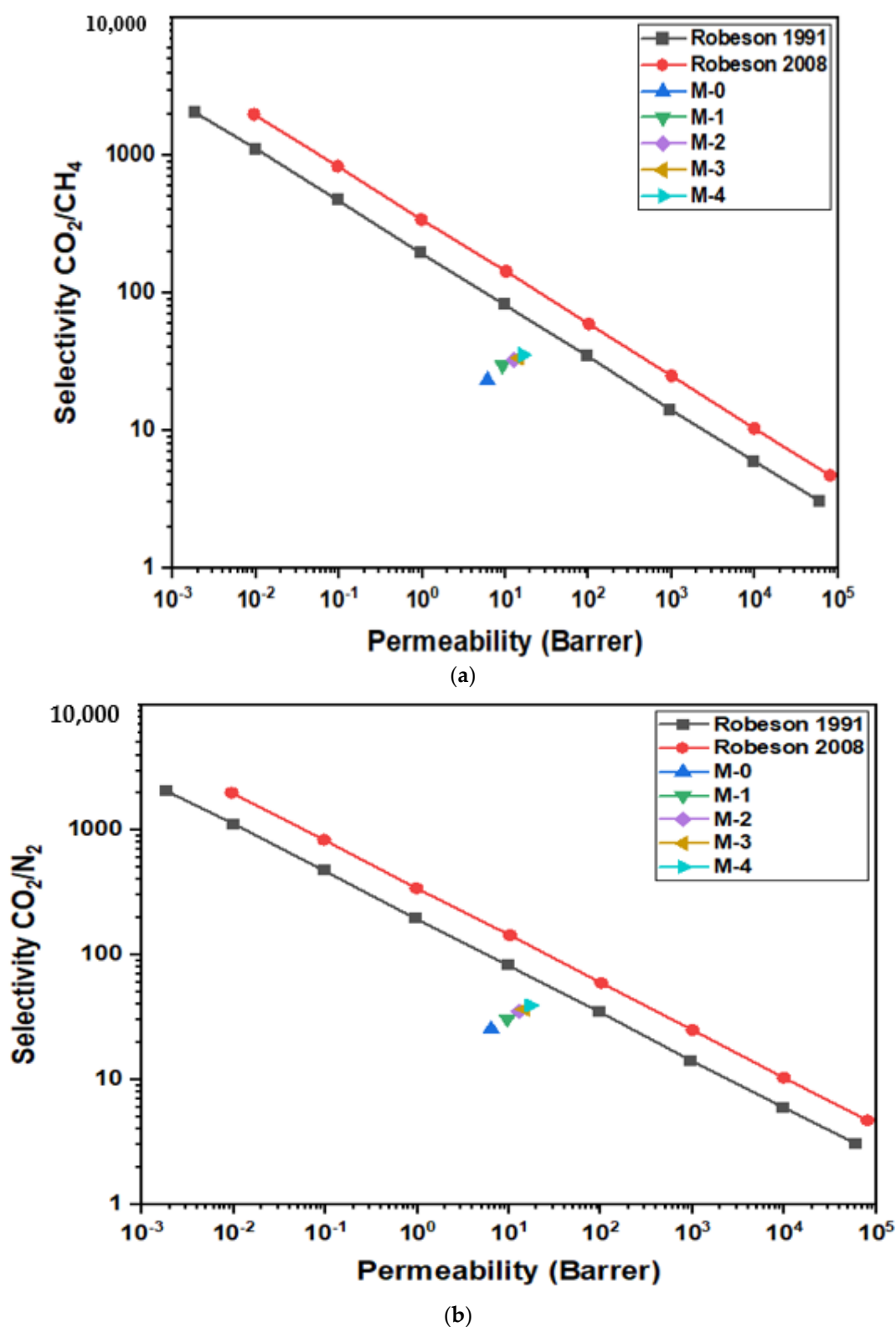


**Figure 5.** (a) Robeson plot comparison of MMMs for mixed gas  $\text{CO}_2/\text{CH}_4$ . (b) Robeson plot comparison of MMMs for mixed gas  $\text{CO}_2/\text{N}_2$ .

### 3. Materials and Methods

#### 3.1. Materials

PSF of A.M.W  $\sim 22,000$ , cetrimonium bromide (CTMB) (Purity  $\geq 98\%$ ), and acetic acid (Purity  $\geq 99\%$ ) were purchased from Sigma-Aldrich (St. Louis, MO, USA). Tetrahydrofuran

(THF) (Purity = 99.6%), isopropyl alcohol (Purity  $\geq$  99.5%), ethylene glycol (Purity = 99%) and acetone (Purity  $\geq$  95%) for washing purposes were purchased from Fisher Scientific. Ammonium cerium (IV) nitrate (Purity = 99.5%) was obtained from Scharlau. A Water Purification Unit (Adrona SIA-B30, Riga, Latvia) is used to obtain Ultrapure water for washing purposes.

### 3.2. Deep Eutectic Solvent (DES) Preparation

The synthesis of DES was reported in our previous publication [33]. Briefly, DES was formed by combining equal masses of cetrimonium bromide (CTMB) and acetic acid at 70 °C for 3 h to obtain a homogeneous mixture. The synthesis was confirmed physically by analyzing the lowering of melting point as compared to the separate constituents and chemically by FTIR analysis. Figure 6 shows that CTMB was the hydrogen bond acceptor (HBA) and acetic acid was the hydrogen bond donor (HBD) [37].

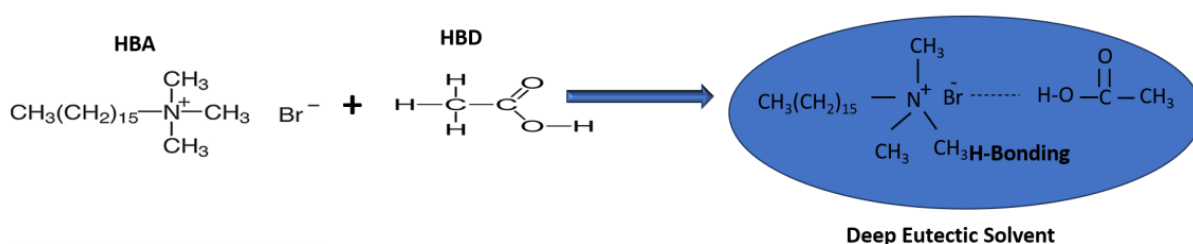


**Figure 6.** Synthesis of DES and H-bonding between CTMB and acetic acid [33].

### 3.3. Ceria Nanoparticles formation

The method of formation of the ceria nanoparticles has already been reported. Briefly, the uniform red-colored solution was formed by adding 0.3 g ammonium cerium (IV) nitrate into a mixture of 10 mL ethylene glycol and 10 mL isopropyl alcohol. The small amount of acetic acid (1 mL) was added to the above mixture dropwise with continuous stirring. The red solution was converted to a uniform colorless solution after 2 h of stirring. A Teflon-lined hydrothermal autoclave was used as a batch reactor and the resultant mixture was placed in an oven at 130 °C for 7 h. The yield was in the form of a greenish-brown mixture when cooled to room temperature. Ceria nanoparticles were obtained by centrifugation of the resultant mixture for 5 min at 8000 rpm. The solvents that were unreacted were recycled to avoid losses. The product was cleaned 3 times with ethanol and 1 time using acetone to achieve dried cerium oxide nanoparticles. After drying, 0.67 g of NPs was formed. In the recycling process, 0.3 g ammonium cerium (IV) nitrate was mixed with the unreacted solvents, then 0.7 mL acetic acid was added to the solution and the same procedure was repeated. The yield was 0.59 g in the first recycling process. In the second recycling process, the same procedure was repeated with 0.5 mL acetic acid and the yield was 0.50 g.

### 3.4. Surface Modification of Cerium Oxide Nanoparticles by DES

The DES-modified cerium oxide NPs were obtained by mixing the NPs with DES with a 8:1 ratio by weight into the small amount of evaporated organic solvent that is ethanol; the agglomeration was reduced using a mortar and pestle before using ethanol. The mixture was stirred to homogenize and placed at room temperature to evaporate the complete solvent for 24 h. The yield obtained after drying, that is the filler for MMMs, was named DES-ceria [33]. The work-flow of the surface tuning of ceria NPs is shown in Figure 7.

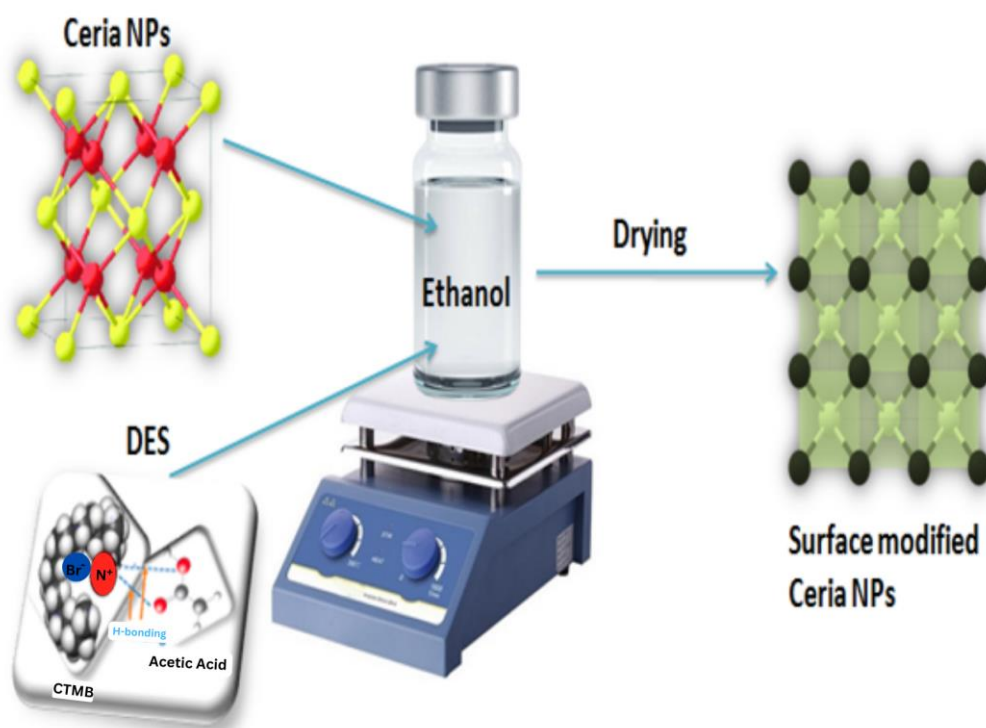


**Figure 7.** Surface tuning of ceria nanoparticles using CTMB-based deep eutectic solvent [33].

### 3.5. Mixed Matrix Membranes Fabrication

MMMs of various filler loadings were synthesized using DES-ceria nanoparticles as a filler with the help of a solution casting technique for dense membrane synthesis as shown in Table 2. PSF was mixed in THF for 2 h in a vial at room temperature with stirring of 500 rpm. After complete dissolution of the PSF, filler was added to the solution and mixed for 24 h under the same conditions to form a uniform composition. The air bubbles were removed using the gravity method and the solution was placed into a flat-bottom petri dish and left for 24 h to dry. After complete solvent evaporation, the membrane was peeled off from the bottom. The whole process of MMM synthesis is shown in Figure 8.

**Table 2.** MMMs composition by weight percentage.

| Membrane Id | Membrane Type     | PSF | Ceria | THF  |
|-------------|-------------------|-----|-------|------|
| M-0         | PSF               | 4.8 | -     | 95.2 |
| M-1         | 2% ceria membrane | 4.8 | 0.1   | 95.1 |
| M-2         | 4% ceria membrane | 4.8 | 0.2   | 95.0 |
| M-3         | 6% ceria membrane | 4.8 | 0.3   | 94.9 |
| M-4         | 8% ceria membrane | 4.8 | 0.4   | 94.8 |

### 3.6. Characterization of Membrane Samples

The Tescan Vega LMU variable pressure Scanning Electron Microscope (Brno-Kohoutovice Czech Republic) was utilized to observe the cross-sectional and surface morphologies of the membrane samples. The Thermo Scientific Nicolet iS5 instrument from the United States was used to conduct the FTIR (Fourier Transform Infrared) spectroscopic analysis of membrane samples. A TGA analyzer (Perkin-Elmer STA 6000, Waltham, MA, USA), was utilized to examine the thermal stability of membrane samples. The composition of gases was evaluated with the help of a gas chromatograph (Agilent 7890, Santa Clara, CA, USA).

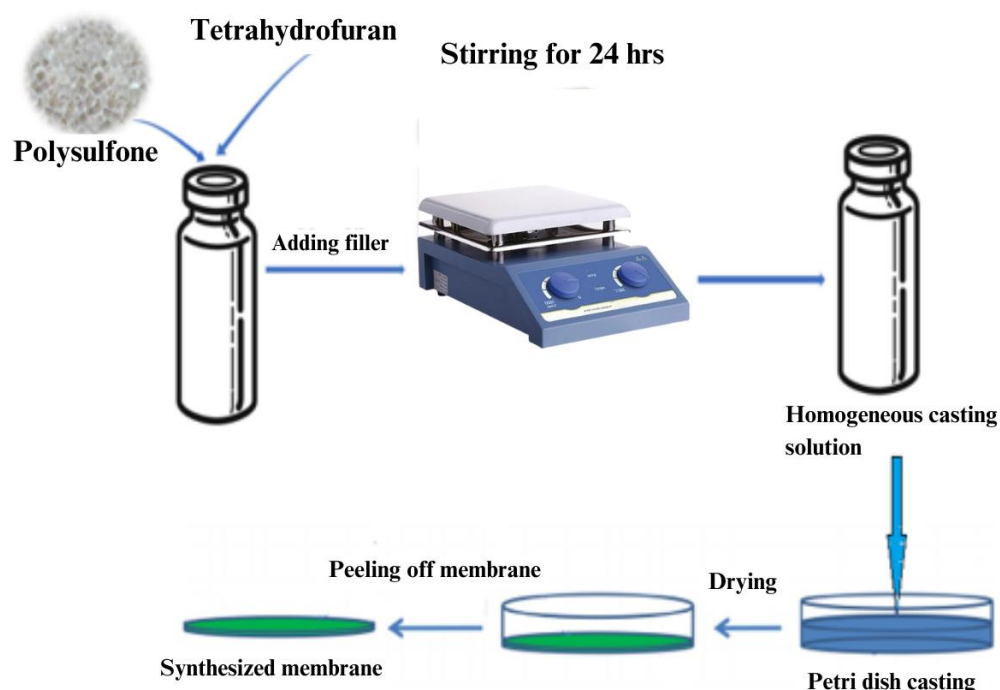


**Figure 8.** Schematic diagram for synthesis of mixed matrix dense membrane [33].

#### 4. Conclusions

Ceria NPs were synthesized and combined with DES to fabricate a novel filler. MMMs of DES-ceria NPs were developed using a solvent evaporation technique. The SEM, FTIR and TGA of the membranes were performed. The SEM micrograph revealed the cross-sectional and surface morphologies of the synthesized MMMs, which described that the DES-ceria NPs were uniformly distributed over the polymer matrix and also making agglomerates because of the magnetic effects among the particles. The FTIR spectra indicated characteristic peaks of all of the constituents that suggests that no chemical reaction took place in the preparation of the membranes as all of the characteristic peaks can be easily indicated with respect to their functional groups. The TGA provided the comparison of thermal stabilities of the membrane and that the membrane with the highest filler loading was the most stable membrane which highlights the thermal stability of DES-ceria NPs, and that the overall trend for thermal stability was ascending from 0% to 8% DES-ceria NPs. The gas permeation analysis was carried out using pure and mixed gases and highlighted the enhanced permeability of CO<sub>2</sub> and the selectivity as compared to a pristine PSF membrane. The improvement in the permeability of CO<sub>2</sub> in pure and mixed gases (CO<sub>2</sub>/CH<sub>4</sub> and CO<sub>2</sub>/N<sub>2</sub>) was from 6.7 Barrer to 17.2 Barrer, from 6.06 Barrer to 16.3 Barrer and from 6.36 Barrer to 16.9 Barrer, respectively. The improvement in the selectivities of the pure gases was from 24.81 to 41.95 (CO<sub>2</sub>/CH<sub>4</sub>) and from 26.8 to 40.95 (CO<sub>2</sub>/N<sub>2</sub>), and for the mixed gases was from 23.31 to 35.43 (CO<sub>2</sub>/CH<sub>4</sub>) and from 25.44 to 39.3 (CO<sub>2</sub>/N<sub>2</sub>). Thus, the DES-ceria NP-based MMMs enhanced the permeability as well as the selectivity and proved to be a promising filler for the mitigation of CO<sub>2</sub> from a gaseous mixture. In future, mathematical modeling can also be applied by obtaining statistical data for different parameters relevant to the presented work, and also further modification of the nanoparticles by tunable DESs can open up a way for CO<sub>2</sub> separation via MMMs.

**Supplementary Materials:** The following supporting information can be downloaded at: <https://www.mdpi.com/article/10.3390/molecules28207162/s1>, Figure S1: Surface images of synthesized membranes; Table S1: The pure gas permeability and ideal gas selectivity of DES-ceria NPs based MMMs; Table S2: The mixed gas permeabilities and selectivities of DES-ceria NPs based MMMs.

**Author Contributions:** S.-u.-R.: Methodology, Writing—Original draft preparation. M.S.M.: Data curation, Supervision. M.J.: Review and Editing. S.U.Z.: Review and Editing. S.R.: Visualization, Investigation. N.M.: Conceptualization. J.b.F.: Validation, Software, M.A.: paper format preparation. M.F.-e.-A.: Review and Editing. J.R.: Review and Editing. M.U.: Review and Editing. R.A.A.: Funding acquisition. S.A.S.: Funding acquisition. All authors have read and agreed to the published version of the manuscript.

**Funding:** This work was funded by the Researchers Supporting Project Number (RSP2023R265), King Saud University, Riyadh, Saudi Arabia, and also supported by the International Islamic University Malaysia Research Management Centre Grant (RMCG20-038-0038).

**Institutional Review Board Statement:** Not Applicable.

**Informed Consent Statement:** Not Applicable.

**Data Availability Statement:** The data will be available on request.

**Conflicts of Interest:** The authors declare no conflict of interest.

**Sample Availability:** Not Applicable.

## References

1. Chuah, C.Y.; Goh, K.; Yang, Y.; Gong, H.; Li, W.; Karahan, H.E.; Guiver, M.D.; Wang, R.; Bae, T.-H. Harnessing filler materials for enhancing biogas separation membranes. *Chem. Rev.* **2018**, *118*, 8655–8769. [\[CrossRef\]](#)
2. Hua, Y.; Wang, H.; Li, Q.; Chen, G.; Liu, G.; Duan, J.; Jin, W. Highly efficient CH<sub>4</sub> purification by LaBTB PCP-based mixed matrix membranes. *J. Mater. Chem. A* **2018**, *6*, 599–606. [\[CrossRef\]](#)
3. Norahim, N.; Yaisanga, P.; Faungnawakij, K.; Charinpanitkul, T.; Klagsom, C. Recent membrane developments for CO<sub>2</sub> separation and capture. *Chem. Eng. Technol.* **2018**, *41*, 211–223. [\[CrossRef\]](#)
4. Xie, K.; Fu, Q.; Qiao, G.G.; Webley, P.A. Recent progress on fabrication methods of polymeric thin film gas separation membranes for CO<sub>2</sub> capture. *J. Membr. Sci.* **2019**, *572*, 38–60. [\[CrossRef\]](#)
5. Olajire, A.A. CO<sub>2</sub> capture and separation technologies for end-of-pipe applications—A review. *Energy* **2010**, *35*, 2610–2628. [\[CrossRef\]](#)
6. Bernardo, P.; Drioli, E.; Golemme, G. Membrane gas separation: A review/state of the art. *Ind. Eng. Chem. Res.* **2009**, *48*, 4638–4663. [\[CrossRef\]](#)
7. Koros, W.J.; Zhang, C. Materials for next-generation molecularly selective synthetic membranes. *Nat. Mater.* **2017**, *16*, 289–297. [\[CrossRef\]](#)
8. Liu, G.; Jin, W.; Xu, N. Two-dimensional-material membranes: A new family of high-performance separation membranes. *Angew. Chem. Int. Ed.* **2016**, *55*, 13384–13397. [\[CrossRef\]](#)
9. Hou, J.; Zhang, H.; Simon, G.P.; Wang, H. Polycrystalline advanced microporous framework membranes for efficient separation of small molecules and ions. *Adv. Mater.* **2020**, *32*, e1902009. [\[CrossRef\]](#)
10. Kosinov, N.; Gascon, J.; Kapteijn, F.; Hensen, E.J. Recent developments in zeolite membranes for gas separation. *J. Membr. Sci.* **2016**, *499*, 65–79. [\[CrossRef\]](#)
11. Anderson, M.; Wang, H.; Lin, Y. Inorganic membranes for carbon dioxide and nitrogen separation. *Rev. Chem. Eng.* **2012**, *28*, 101–121. [\[CrossRef\]](#)
12. Wang, S.; Li, X.; Wu, H.; Tian, Z.; Xin, Q.; He, G.; Peng, D.; Chen, S.; Yin, Y.; Jiang, Z.; et al. Advances in high permeability polymer-based membrane materials for CO<sub>2</sub> separations. *Energy Environ. Sci.* **2016**, *9*, 1863–1890. [\[CrossRef\]](#)
13. Galizia, M.; Chi, W.S.; Smith, Z.P.; Merkel, T.C.; Baker, R.W.; Freeman, B.D. 50th anniversary perspective: Polymers and mixed matrix membranes for gas and vapor separation: A review and prospective opportunities. *Macromolecules* **2017**, *50*, 7809–7843. [\[CrossRef\]](#)
14. Robeson, L.M. The upper bound revisited. *J. Membr. Sci.* **2008**, *320*, 390–400. [\[CrossRef\]](#)
15. Dechnick, J.; Gascon, J.; Doonan, C.J.; Janiak, C.; Sumby, C. Mixed-matrix membranes. *Angew. Int. Ed.* **2017**, *56*, 9292–9310. [\[CrossRef\]](#) [\[PubMed\]](#)
16. Cheng, Y.; Wang, Z.; Zhao, D. Mixed matrix membranes for natural gas upgrading: Current status and opportunities. *Ind. Eng. Chem. Res.* **2018**, *57*, 4139–4169. [\[CrossRef\]](#)
17. Dorosti, F.; Omidkhah, M.; Abedini, R. Fabrication and characterization of Matrimid/MIL-53 mixed matrix membrane for CO<sub>2</sub>/CH<sub>4</sub> separation. *Chem. Eng. Res. Des.* **2014**, *92*, 2439–2448. [\[CrossRef\]](#)



18. Sadeghi, Z.; Omidkhah, M.; Masoumi, M.E.; Abedini, R. Modification of existing permeation models of mixed matrix membranes filled with porous particles for gas separation. *Can. J. Chem. Eng.* **2016**, *94*, 547–555. [\[CrossRef\]](#)
19. Jamshidi, M.; Pirouzfard, V.; Abedini, R.; Pedram, M.Z. The influence of nanoparticles on gas transport properties of mixed matrix membranes: An experimental investigation and modeling. *Korean J. Chem. Eng.* **2017**, *34*, 829–843. [\[CrossRef\]](#)
20. Zhang, S.; Zhang, J.; Zhang, Y.; Deng, Y. Nanoconfined ionic liquids. *Chem. Rev.* **2017**, *117*, 6755–6833. [\[CrossRef\]](#)
21. Liu, Y.; Wu, H.; Wu, S.; Song, S.; Guo, Z.; Ren, Y.; Zhao, R.; Yang, L.; Wu, Y.; Jiang, Z. Multifunctional covalent organic framework (COF)-Based mixed matrix membranes for enhanced CO<sub>2</sub> separation. *J. Membr. Sci.* **2021**, *618*, 118693. [\[CrossRef\]](#)
22. Wang, M.; Wang, Z.; Zhao, S.; Wang, J.; Wang, S. Recent advances on mixed matrix membranes for CO<sub>2</sub> separation. *Chin. J. Chem. Eng.* **2017**, *25*, 1581–1597. [\[CrossRef\]](#)
23. Kim, S.; Lee, Y.M. High performance polymer membranes for CO<sub>2</sub> separation. *Curr. Opin. Chem. Eng.* **2013**, *2*, 238–244. [\[CrossRef\]](#)
24. Aroon, M.; Ismail, A.; Matsuura, T.; Montazer-Rahmati, M. Performance studies of mixed matrix membranes for gas separation: A review. *Sep. Purif. Technol.* **2010**, *75*, 229–242. [\[CrossRef\]](#)
25. Hasebe, S.; Aoyama, S.; Tanaka, M.; Kawakami, H. CO<sub>2</sub> separation of polymer membranes containing silica nanoparticles with gas permeable nano-space. *J. Membr. Sci.* **2017**, *536*, 148–155. [\[CrossRef\]](#)
26. Raouf, M.; Abedini, R.; Omidkhah, M.; Nezhadmoghadam, E. A favored CO<sub>2</sub> separation over light gases using mixed matrix membrane comprising polysulfone/polyethylene glycol and graphene hydroxyl nanoparticles. *Process. Saf. Environ. Prot.* **2020**, *133*, 394–407. [\[CrossRef\]](#)
27. Sainath, K.; Modi, A.; Bellare, J. In-situ growth of zeolitic imidazolate framework-67 nanoparticles on polysulfone/graphene oxide hollow fiber membranes enhance CO<sub>2</sub>/CH<sub>4</sub> separation. *J. Membr. Sci.* **2020**, *614*, 118506. [\[CrossRef\]](#)
28. Ruhaimi, A.H.; Ab Aziz, M.A. Spherical CeO<sub>2</sub> nanoparticles prepared using an egg-shell membrane as a bio-template for high CO<sub>2</sub> adsorption. *Chem. Phys. Lett.* **2021**, *779*, 138842. [\[CrossRef\]](#)
29. Farashi, Z.; Azizi, S.; Arzhandi, M.R.D.; Noroozi, Z.; Azizi, N. Improving CO<sub>2</sub>/CH<sub>4</sub> separation efficiency of Pebax-1657 membrane by adding Al<sub>2</sub>O<sub>3</sub> nanoparticles in its matrix. *J. Nat. Gas Sci. Eng.* **2019**, *72*, 103019. [\[CrossRef\]](#)
30. Xu, R.; Wang, Z.; Wang, M.; Qiao, Z.; Wang, J. High nanoparticles loadings mixed matrix membranes via chemical bridging-crosslinking for CO<sub>2</sub> separation. *J. Membr. Sci.* **2019**, *573*, 455–464. [\[CrossRef\]](#)
31. Taghizadeh, M.; Taghizadeh, A.; Vatanpour, V.; Ganjali, M.R.; Saeb, M.R. Deep eutectic solvents in membrane science and technology: Fundamental, preparation, application, and future perspective. *Sep. Purif. Technol.* **2020**, *258*, 118015. [\[CrossRef\]](#)
32. Jablonský, M.; Škulcová, A.; Šima, J. Use of deep eutectic solvents in polymer chemistry—A review. *Molecules* **2019**, *24*, 3978. [\[CrossRef\]](#)
33. Reed, K.; Cormack, A.; Kulkarni, A.; Mayton, M.; Sayle, D.; Klaessig, F.; Stadler, B. Exploring the properties and applications of nanoceria: Is there still plenty of room at the bottom? *Environ. Sci. Nano* **2014**, *1*, 390–405. [\[CrossRef\]](#)
34. Feng, Y.; Han, G.; Chung, T.-S.; Weber, M.; Widjojo, N.; Maletzko, C. Effects of polyethylene glycol on membrane formation and properties of hydrophilic sulfonated polyphenylenesulfone (sPPSU) membranes. *J. Membr. Sci.* **2017**, *531*, 27–35. [\[CrossRef\]](#)
35. Elahi, B.; Mirzaee, M.; Darroudi, M.; Oskuee, R.K.; Sadri, K.; Amiri, M.S. Preparation of cerium oxide nanoparticles in *Salvia Macrosiphon* Boiss seeds extract and investigation of their photo-catalytic activities. *Ceram. Int.* **2019**, *45*, 4790–4797. [\[CrossRef\]](#)
36. Sreekanth, T.; Dillip, G.; Lee, Y.R. Picrasmaquassioides mediated cerium oxide nanostructures and their post-annealing treatment on the microstructural, morphological and enhanced catalytic performance. *Ceram. Int.* **2016**, *42*, 6610–6618. [\[CrossRef\]](#)
37. Zhang, Q.; De Oliveira Vigier, K.; Royer, S.; Jérôme, F. Deep eutectic solvents: Syntheses, properties and applications. *Chem. Soc. Rev.* **2012**, *41*, 7108–7146. [\[CrossRef\]](#)
38. Shahbaz, K.; Mjalli, F.S.; Hashim, M.A.; AlNashef, I.M. Using deep eutectic solvents based on methyl triphenyl phosphonium bromide for the removal of glycerol from palm-oil-based biodiesel. *Energy Fuels* **2011**, *25*, 2671–2678. [\[CrossRef\]](#)
39. Durand, E.; Lecomte, J.; Villeneuve, P. Deep eutectic solvents: Synthesis, application, and focus on lipase-catalyzed reactions. *Eur. J. Lipid Sci. Technol.* **2013**, *115*, 379–385. [\[CrossRef\]](#)
40. Lian, S.; Li, R.; Zhang, Z.; Liu, Q.; Song, C.; Lu, S. Improved CO<sub>2</sub> separation performance and interfacial affinity of composite membranes by incorporating amino acid-based deep eutectic solvents. *Sep. Purif. Technol.* **2021**, *272*, 118953. [\[CrossRef\]](#)
41. Muduli, S.K.; Wang, S.; Chen, S.; Ng, C.F.; Huan, C.H.A.; Sum, T.C.; Soo, H.S. Mesoporous cerium oxide nanospheres for the visible-light driven photocatalytic degradation of dyes. *Beilstein J. Nanotechnol.* **2014**, *5*, 517–523. [\[CrossRef\]](#)
42. Yang, L.; Zhang, S.; Wu, H.; Ye, C.; Liang, X.; Wang, S.; Wu, X.; Wu, Y.; Ren, Y.; Liu, Y.; et al. Porous organosilicon nanotubes in pebax-based mixed-matrix membranes for biogas purification. *J. Membr. Sci.* **2019**, *573*, 301–308. [\[CrossRef\]](#)
43. Singh, K.; Devi, S.; Bajaj, H.C.; Ingole, P.; Choudhari, J.; Bhrambhath, H. Optical resolution of racemic mixtures of amino acids through nanofiltration membrane process. *Sep. Sci. Technol.* **2014**, *49*, 2630–2641. [\[CrossRef\]](#)
44. Shan, M.; Seoane, B.; Andres-Garcia, E.; Kapteijn, F.; Gascon, J. Mixed-matrix membranes containing an azine-linked covalent organic framework: Influence of the polymeric matrix on post-combustion CO<sub>2</sub>-capture. *J. Membr. Sci.* **2018**, *549*, 377–384. [\[CrossRef\]](#)
45. Chen, Y.; Ho, W.W. High-molecular-weight polyvinylamine/piperazine glycinate membranes for CO<sub>2</sub> capture from flue gas. *J. Membr. Sci.* **2016**, *514*, 376–384. [\[CrossRef\]](#)
46. Khan, A.L.; Basu, S.; Cano-Odena, A.; Vankelecom, I.F. Novel high throughput equipment for membrane-based gas separations. *J. Membr. Sci.* **2010**, *354*, 32–39. [\[CrossRef\]](#)



47. Robeson, L.M. Correlation of separation factor versus permeability for polymeric membranes. *J. Membr. Sci.* **1991**, *62*, 165–185. [[CrossRef](#)]
48. Vakharia, V.; Salim, W.; Wu, D.; Han, Y.; Chen, Y.; Zhao, L.; Ho, W.W. Scale-up of amine-containing thin-film composite membranes for CO<sub>2</sub> capture from flue gas. *J. Membr. Sci.* **2018**, *555*, 379–387. [[CrossRef](#)]

**Disclaimer/Publisher’s Note:** The statements, opinions and data contained in all publications are solely those of the individual author(s) and contributor(s) and not of MDPI and/or the editor(s). MDPI and/or the editor(s) disclaim responsibility for any injury to people or property resulting from any ideas, methods, instructions or products referred to in the content.